

Determining the Turning Wing Kinematics of a Ruby-Throated Hummingbird

Thomas Massion and Jialei Song

KEYWORDS. Micro Aerial Vehicles, blade element model, computational fluid dynamics

BRIEF. The turning wing kinematics of a ruby-throated hummingbird are determined by use of a blade element model.

ABSTRACT. A new field of engineering involving small unmanned automated flying vehicles called Micro Aerial Vehicles (MAVs) is emerging with applications such as small-scale surveillance for the military. The most recent and promising model for MAVs involves modeling insect-like flyers such as hummingbirds due to their unique mode of flight that includes the ability to hover and fly backwards unlike many other birds, yet all the while maintaining capabilities for complex in-flight maneuvers. In order to further understanding of this insect-like flight for future biomimetic application, the turning wing kinematics of a ruby-throated hummingbird were determined. In this study, video from a ruby-throated hummingbird is used to extract data points from which variables for a translational force, rotational force, and force due to acceleration effect can be solved so that the overall torque can be found to describe the mechanism of the hummingbird's turning. A blade element model or (BEM) approach is used which involves breaking the wing down into a series of strips or "blades" that have their own forces. The wing forces and torque that drive the hummingbird's turning were successfully solved for, and a direction towards finding the mechanism of the hummingbird's turning was determined.

INTRODUCTION.

In the world of engineering, a new field has recently emerged with its focus on developing insect-sized robots known as Micro Aerial Vehicles (MAVs). The main practical application proposed for these robots has been small scale military scenarios in which MAVs could execute missions in complex environments with stealth. For example, an MAV could be used for quick surveillance in small areas if applied with video, and with its minute size could find its way into a room occupied by hostile forces whose presence was previously unknown, thereby preventing an ambush. Also, in accordance with radioactive or chemical detection technology, MAVs of the future could also be used on the battlefield or in a disaster scenario to prevent harmful exposure from biochemical or radioactive hazards [1].

Of the various recent models for MAVs, the most promising of these models have been those involving flapping wings. Compared to those models with rotary propellers or fixed wings, flapping wings have been advantageous in terms of flight efficiency, maneuverability as the size becomes smaller, in which case the Reynolds number, a measure of how flow patterns will behave on a certain scale, is very low [2]. The basis for flapping wings came from the flyers of this scale in nature such as insects and small birds. Hummingbirds have been especially advantageous in this respect due to their superior flight performance. They have shown to be capable of sustainable hovering, flying forward at high speeds, sharp turns, and flying upside-down for short periods.

Using hummingbirds as a model, however, means that the various factors involved in creating the forces that generate their flight must be understood. There have recently been two major computational-modeling approaches in determining such characteristics: a low fidelity and high fidelity model in which the terms "high fidelity" and "low fidelity" respectively describe the accuracy of a model. The low fidelity model in this case has consisted of a quasi-steady blade element model (BEM). A previous study by Song et al has shown that the quasi-steady model generally succeeds in predicting overall forces production although it overlooks some of the unsteady effects that the flow-field, or collection of freely moving air particles surrounding an object, has on the hum-

mingbird during flight [3]. However, the less computationally taxing nature of quasi-steady modeling and capability to nevertheless yield fairly accurate measurements has made it a prevalent and promising method. Comparatively, the high fidelity model would consist of a computational fluid dynamics (CFD) approach which would describe force characteristics as in the BEM while furthermore accounting for flow field configuration by using the Navier-Stokes equations [4]. The trade-off here has existed with the high amount of computing effort and time needed to complete a CFD model. More specifically, a previous study also by Song et al created a CFD model looking at the hovering aspect of a ruby-throated hummingbird's flight showed that there exist other factors not accounted for in the quasi-steady model that contribute to the lift of the bird [4].

This study set out to use a low-fidelity BEM model with a kinematic approach similar to that of Song et al to quantify and characterize specifically the turning aspect of a hummingbird's flight from a hovering stage [3]. This data would advance the field's comprehension of the hummingbird's flight so that more flight-efficient MAVs could be developed in the future.

MATERIALS AND METHODS.

Wing Kinematic Reconstruction.

In characterizing the ruby-throated hummingbird's flight, a wing kinematic reconstruction was done so that computational measures could be taken with ease. First, high-speed videos of the hummingbird were acquired. Before taking the video of the hummingbird in flight, nine white markers had been dotted on the edge of the wing to ensure consistency in the digitization of the wing on each frame. Four visible high-speed cameras and two thermal IR cameras, all having a camera frequency of 1000 Hz, were used to film the hummingbird flight in the wind tunnel and to locate wing markers while minimizing blind spots. Using a free digitization software, the markers from the high speed videos on the wing were digitized frame by frame to obtain the three dimensional position of each marker.

The digitized points from the nine markers were then used to make a full three dimensional kinematic reconstruction. In this reconstruction, new points were interpolated and a finite element mesh was generated in MATLAB to define the entire wing surface. Spline interpolation was used in the time domain to interpolate more frames and smooth results. In total, there were 700 three dimensional points resulting from spline interpolation and smoothing that were used to describe the wings for 2000 time-steps which were later used for determining model parameters. To give some perspective, one time-step here would be equal to 0.145 milliseconds, and the entire time-span of the video that was analyzed lasted about 0.29 seconds.

Force Calculation.

The turning of the hummingbird is generally the consequence of torque discrepancy between the two wings, due to their asymmetric motion. Researchers have generally suspected that birds and insects primarily use an asymmetry in the angle of attack, flapping frequency or flapping amplitude to generate the torque asymmetry [3]. In order to determine which factors cause the torque asymmetry, a blade element model (BEM) was adopted in this study to quantitatively calculate the force and torque production based on the wing kinematics. This quantitative approach consists of breaking the wing down into several strips or "blades" and summing the forces from each to attain the total force

on the wing. In the following equations, these “blades” are mathematically described using “chord” lengths and angles for consistency with previous literature. There are three fundamental forces generated by each blade of each wing: the translational force, rotational force, and force due to the acceleration-effect. Eq. 1 depicts the translational force:

$$\mathbf{F}_{trans} = \frac{\rho \dot{\Phi}^2 R^3 \bar{c}}{2} \int_0^1 \hat{r}^2 \hat{c} \begin{bmatrix} C'_D(\alpha) \\ C'_L(\alpha) \end{bmatrix} d\hat{r} \quad (1)$$

where ρ , was the air density, $\dot{\Phi}$, was the instantaneous angular velocity of the wing, \hat{r} , was the dimensionless span-wise location scaled by R ; \hat{c} was the dimensionless chord length according to \bar{c} ; $C'_D(\alpha)$ is the drag coefficient and $C'_L(\alpha)$ is the lift coefficient. Both C'_D and C'_L are dependent upon the angle of attack α . In order to obtain the relation between these force coefficients and the angle of attack, a series of revolving wing CFD simulation with constant angle of attacks were previously run. The force found on the wing from this simplified CFD model with an assumed steady-state was used to fit the data, and the fitted relations are shown in Eq. 2 and Eq. 3[3].

$$C'_D = 0.245 + 1.63 \sin(2.43\alpha - 6.3^\circ) \quad (2)$$

$$C'_L = 1.88 - 1.70 \cos(2.27\alpha - 10.66^\circ) \quad (3)$$

These calibrated coefficients based on CFD could therefore most accurately correlate the two variables [2]. The total translational force is the resultant vector of the lift and drag forces [3].

$$\mathbf{F}_{rot} = C_{rot} \rho \dot{\Phi} \bar{c}^2 R^2 \int_0^1 \hat{r} \hat{c}^2 \dot{\alpha} \mathbf{n} d\hat{r} \quad (4)$$

The rotational force is shown in Eq. 4 where $\dot{\alpha}$ is the instantaneous pitching velocity, and \mathbf{n} is the surface normal which was assumed to be orthogonal to the chord surface. C_{rot} is the rotational force coefficient dependent on the location of the pitching axis, which is represented by dimensionless distance from the leading edge assumed to be 0.25 in the equation $C_{rot} = \pi(0.75)$. Previous researchers have found that the value 0.25 for \hat{r} has consistently been the case for most insect-like flyers such as the fruit fly, hawk moth, and hummingbird [2].

The force due to the acceleration effect is given in Eq. (5):

$$\mathbf{F}_{acc} = \frac{\rho \pi \bar{c}^2 R^2}{4} \int_0^1 \hat{r} \hat{c}^2 [\ddot{\Phi} \sin \alpha + \dot{\Phi} \dot{\alpha} \cos \alpha] \mathbf{n} d\hat{r} + \frac{\rho \pi R \bar{c}^2 \ddot{\alpha}}{53} \int_0^1 \hat{c}^3 \mathbf{n} d\hat{r} \quad (5)$$

where $\ddot{\Phi}$ and $\ddot{\alpha}$ were the instantaneous stroke acceleration and pitching acceleration [3]. The normal surface \mathbf{n} was assumed to be orthogonal to the chord surface in this equation [3]. This assumption in respect to the normal surface was made with respect to the acceleration effect force and the vertical force. These forces related back to an overall force vector on the wing that has a certain direction. The predominant force that would significantly change the direction of the resultant force vector on the wing of the hummingbird to more or less than 90 degrees would be due to viscous drag. However, with a moving body at this scale, the Reynold's number which describes the ratio of pressure forces to viscous forces based on the scale of linear dimension determines that the pressure drag would be dominant, making the viscous drag negligible.

These three forces are all decomposed into their vertical and horizontal components. The translational force is decomposed using the tip angle θ , the angle that the tip trajectory makes with a horizontal plane. The rotational force and force due to acceleration effect are decomposed using the chord angle γ , the angle

that the chord makes with a horizontal plane. The decomposition into vertical and horizontal components for the drag and lift components which combine to make the translational force as well as that of the rotational and acceleration-effect forces are shown in Eq. 6 – Eq. 15.

$$dF_{rot,ver} = dF_{rot} \cos \gamma \quad (6)$$

$$dF_{rot,hor} = dF_{rot} \sin \gamma \quad (7)$$

$$dF_{acc,ver} = dF_{acc} \cos \gamma \quad (8)$$

$$dF_{acc,hor} = dF_{acc} \sin \gamma \quad (9)$$

$$dF_{trans_L,hor} = dF_{trans_L} \sin \theta \quad (10)$$

$$dF_{trans_L,ver} = dF_{trans_L} \cos \theta \quad (11)$$

$$dF_{trans_D,hor} = dF_{trans_D} \sin \theta \quad (12)$$

$$dF_{trans_D,ver} = dF_{trans_D} \cos \theta \quad (13)$$

$$dF_{trans,ver} = dF_{trans_L,ver} - dF_{trans_D,ver} \quad (14)$$

$$dF_{trans,hor} = dF_{trans_L,hor} - dF_{trans_D,hor} \quad (15)$$

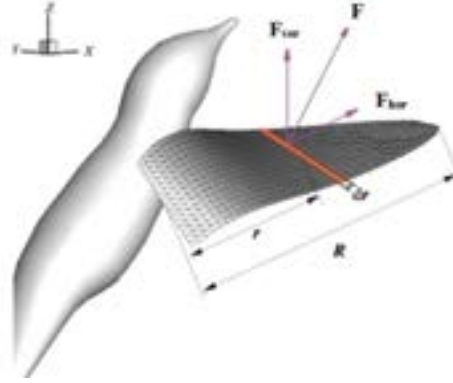


Figure 1. A visual representation of the various parameters described in the methodology is shown. The highlighted region indicates what can be referred to as a “blade” in the blade element model (BEM).

The rotational and acceleration-effect forces were assumed to be perpendicular to the chord angle, which is the angle made by an individual blade of the bird's wing and a horizontal plane, and thus the chord angle can be used to decompose these.

$$dF_{hor} = dF_{trans,hor} + dF_{rot,hor} + dF_{acc,hor} \quad (16)$$

$$dF_{ver} = dF_{trans,ver} + dF_{rot,ver} + dF_{acc,ver} \quad (17)$$

$$\vec{T} = \int d\mathbf{r} \times d\mathbf{F}_{hor} \quad (18)$$

Using the combined horizontal force of each blade dF_{hor} from Eq. 16 the torque is then calculated as shown in Eq. 18.

The BEM in this study makes the quasi-steady assumption which assumes calm fluid surroundings, eliminating the possibility for force interactions that come from anything besides the hummingbird's own doing. As previously mentioned, this then allows one to focus solely on the bird and segment the wing into finite regions as shown in Fig 1, where a respective force is calculated for each region. One limitation of the BEM is the assumption that the wing is a perfect two dimensional object, such that the rigid body dynamics and effects of the different solid properties are not taken into account. Moreover, the BEM used in this study does not take into account the various possible vortex and wake interactions that could be involved in the turning motion of the hummingbird as would a CFD model. However, the advantages of the BEM approach lie heavily in its ability to predict the average overall forces with relative accuracy and computational ease. Research done by Song et al reported the use of the quasi-steady model for calculating the hovering motion of hummingbirds [3].

RESULTS.

Using the previously explained methodology, the necessary angles, forces, and torque values were successfully found. Of the translational, rotational, and acceleration effect forces, the rotational and acceleration-effect forces proved to be so small that they were insignificant in comparison to the translational force when contributing to the overall horizontal or vertical forces.

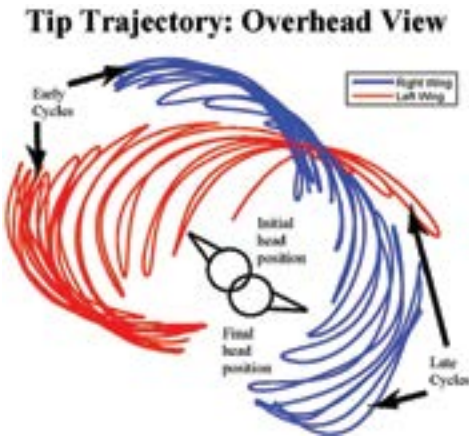


Figure 2. This figure depicts the path taken by the tip of each wing throughout the time segment analyzed from the video as an illustration of the hummingbird's movement. It can be seen from this figure that the bird flapped significantly more in the early cycles to initiate the turn to its right.

The turning of the hummingbird to its right is demonstrated by Fig. 2. Also, the combined vertical force from each wing was equal to the approximate weight of the ruby-throated hummingbird used in this study implying that the BEM model was correct on the average force production.

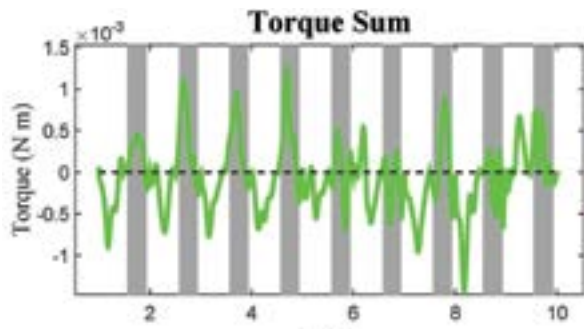


Figure 3. The torque vector sum of the left and right wing is shown here. The shaded region indicates the time period for the down stroke, and the unshaded region indicates the upstroke.

The overall average torque as a sum of the left and right wing is shown in Fig 3. Individually, the torque for the right wing is 6.66×10^{-5} Nm while the average for the left is -1.25×10^{-4} Nm. Thus, the left wing has a larger magnitude in torque than the right wing, and the torque vector sum is -5.8410×10^{-4} Nm.

DISCUSSION.

Each type of wing force was found, decomposed, and then successfully used to find the overall torque for each wing. Results show that the combination of the vertical force from each wing of the hummingbird is approximately equal to the weight of the hummingbird. Therefore, the fundamental fact that the bird can sustain itself in the air was accurately described by the methodology of this study and can verify the accuracy of the rest of the study's findings in comparison to similar or more intensive models.

The results that would aid to describe the underlying cause of the hummingbird's motion have shown to be contrary to the intuitive expectation. Since the hummingbird is turning to its right, one would expect the down stroke of the right wing or the upstroke of the left wing to produce the greatest amount of torque to drive the motion. This domination of a certain period of a wing's flapping would imply that throughout the cycles of wing flapping shown, there would be an overall more positive torque coming from the right wing than from the left wing. However, the extracted forces show that the overall torque for the left wing was more positive than that for the right wing.

A potential explanation to account for this unexpected result could be due to the use of the quasi-steady assumption. The problematic use of this assumption would imply that the more complex fluid interactions not taken into account had a significant effect on producing the torque for the hummingbird. The unseen effect of these fluid interactions would be contrary to previous studies in which the complex fluid interactions acted so that the quasi-steady model was generally successful and further detailed by more complex CFD analysis [3]. In this sense, a complete CFD model on the turning hummingbird could reveal vortex effects that take away from fluid air pushing on the left wing resulting in a torque that corresponds to the bird's change in direction. Another possibility for the results of this study indicating that the left wing has a more positive torque could be that the part of the bird's turning that was digitized for force calculation was incomplete. In order for the hummingbird to make a turn, it requires a positive torque that will initiate the turn and a negative torque that will stop its momentum so that the bird does not continue to turn past what is desired. The concern for this study would be that what was digitized accounted for mainly the negative torque part of the turning and not enough of the positive torque that initiates the turning. In order to correct this digitization, significantly more of the earlier frames of the hummingbird video would need to be digitized.

To resolve these possibilities, a full CFD model of the turning hummingbird must be completed. Use of a CFD model would allow one to identify flow-field interaction as well as potential wing wake interaction and vortex effects such that the air movement and turbulence produced by the wing goes to take effect on the wing itself. Also, it would be necessary to go back and digitize more frames before and after the cycles that have already been analyzed. This way one could hopefully identify the positive and negative torque segments of the bird's turning.

Future studies would also include accounting for the subtleties that exist in fields such as solid body dynamics which include the effects of the composition of the wing on the wing's production of force, potentially adding to the understanding of the turning motion of the hummingbird from hovering. Once the turning of the hummingbird is fully understood, studies examining forward flight and in-flight turning can also add to knowledge of the hummingbird's flight. All of these will contribute to the development of more efficient flight for MAVs.

ACKNOWLEDGMENTS.

I would like to thank all of my instructors at the SSMV and especially my adviser Dr. Stephanie Weeden-Wright for her guidance and helping me attain the opportunity to do this research. I would like to thank Tyson Hedrick for his contribution of the high-speed video. I would also like to thank Dr. Haoxiang Luo for having me in his lab and a very special thanks to my mentor Jialei Song for his countless explanations and patience. Without all of these people, this insightful learning experience would not have been possible.

REFERENCES:

1. T.J. Mueller, J.D. Delaurier. (2001) "Fixed and Flapping Wing Aerodynamics for Micro Air Vehicle Applications." *American Institute of Aeronautics and Astronautics*, vol. 195 pp. 3.W. F. Brinkman, J. Low Temp. Phys. 27, 683 (1977).
2. S.P. Sane, M.H. Dickinson. (2002) "The aerodynamic effects of wing rotation and a revised quasi-steady model of flapping flight." *Journal of Experimental Biology*, vol. 205, pp. 1087-1096.
3. Song J., Luo H., Hedrick T.L. (2015) "Performance of a quasi-steady model for hovering hummingbirds." *Theoretical and Applied Mechanics Letters*, vol. 5 pp 50-53.
4. Song J., Luo H., Hedrick T.L. (2014) "Three-dimensional flow and lift characteristics of a hovering ruby-throated hummingbird." *J. R. Soc. Interface*, 11: 20140541.
5. Luca Petricca, Per Ohlckers, and Christopher Grinde, (2011) "Micro- and Nano-Air Vehicles: State of the Art," *International Journal of Aerospace Engineering*, vol. 2011, pp. 1-17 Article ID: 214549.



Thomas Massion attends Hume-Fogg Academic High School in Nashville, Tennessee; he attended the School for Science and Math at Vanderbilt.